Journal of Molecular Modeling (2022) 28:389
https://doi.org/10.1007/s00894-022-05383-6

ORIGINAL PAPER

Theoretically unveiling the effect of solvent polarities on ESDPT mechanisms and photophysical properties of hydroxyanthraquinones

Xin Xu[1] · Zeran Zhang[1] · Yajie Zhang[1] · Linyue Jin[1] · Qian Cheng[1] · Fang Liu[1] · Chaofan Sun[1]

Received: 7 September 2022 / Accepted: 9 November 2022 / Published online: 16 November 2022

Abstract

In this work, we were devoted to explore the effect of solvent polarities on the excited-state intramolecular proton transfer (ESIPT) process of 1-acetamido-4-hydroxyanthraquinone (AcHAQ) in three different polarity solvents (acetonitrile, chloroform, and cyclohexane) based on the density functional theory (DFT) and time-dependent DFT (TD-DFT) methods, and thereby regulating the distribution ratio between the dual excited-state isomers (enol and keto). The calculated geometrical parameters and infrared (IR) vibrational spectra have confirmed the excited-state intramolecular hydrogen bond (IHB) strengthening mechanism. Natural bond orbital (NBO) population analysis indicates that the intramolecular charge transfer (ICT) around IHBs has enhanced IHB, thereby triggering the ESIPT reaction. In addition, results obtained from the scanned potential energy curve (PEC) manifest that ESIPT process prefers to occur along the O_3-H_2···O_1 IHB and energy barriers corresponding to the proton transfer in ACN are the lowest among all the studied solvents.

Keywords Hydrogen bond · Solvent polarity · ESIPT · TD-DFT · PES

Introduction

Since most organic molecules can only emit a single fluorescence peak, their applications in many fields such as chemistry, physics, and biology are very limited [1–4]. However, organic chromophores with excited-state intramolecular proton transfer (ESIPT) properties often emit double fluorescence peaks in experiments, with larger stokes shifts and higher detection sensitivity and fluorescence quantum yields, which makes them have great development potential in the fields of fluorescent materials, luminescent materials, and molecular logic gates [5–8]. It is well accepted that molecules with ESIPT properties are susceptible to the solvent environment [9–12]. Hence, the energy barrier of proton transfer can be effectively changed by adjusting the polarity of the solvent to achieve the ultimate goal of regularly regulating the fluorescence characteristics and providing effective help for developing new organic light-emitting materials and fluorescent probes [13–16].

In 2018, Zhang and colleagues experimentally synthesized the HBT-H, which is a derivative of 2-(2-hydroxyphenyl)benzothiazole (HBT) [17]. By measuring a large number of absorption and fluorescence spectra in many solvents with different polarities, solvatochromic effect was investigated in detail. Regrettably, experimental spectroscopic techniques often fail to give direct information on photophysical, photochemical, and geometric structures, so they do not discuss in detail why HBT-H behaves differently. Later, Yang et al. investigated for the first time the solvent-induced discoloration effect of HBT-T and the reaction mechanism of proton transfer within the excited-state molecule based on density functional theory (DFT) and time-dependent density functional theory (TD-DFT) and gave a proper quantum-level explanation [18]. Moreover, they reproduced the experimentally observed photophysical phenomena by simulating the absorption and emission spectra of molecules. The qualitative effect of solvent polarity on molecular charge transfer excitation was also found by observing the distribution of electron clouds on frontier molecular orbital (FMO), and the solvent-degenerate effect of molecules was revealed in theoretical detail.

✉ Fang Liu
1421372717@qq.com

✉ Chaofan Sun
cfsun@nefu.edu.cn

[1] College of Science, Northeast Forestry University, Harbin 150040, Heilongjiang, China

Compared with ordinary organic molecules with single fluorescence emission, molecules with dual fluorescence emission and significant stokes shift characteristics tend to have more research value and development potential [19–21]. Numerous previous studies have confirmed that the photophysical properties of ESIPT systems are sensitive to the polarity of surrounding solvents. Therefore, it is a good option to adjust the luminescence properties by changing the solvent polarity without changing the molecular structure for ESIPT chromophores [22–24]. In this study, we not only sought to find the most suitable computational level for the molecule under study by combining theory with experiments but also established the relationship between solvent polarity, intramolecular hydrogen bond (IHB) strength, and ESIPT energy barriers.

Up to now, there is no report on the influence of ESIPT properties of the 1-acetylamino-4-hydroxyanthraquinone molecule (AcHAQ). Based on this, we take AcHAQ as the research object and systematically study the influence of solvent polarity on its ESIPT reaction process based on DFT and TD-DFT. Three aprotic solvents, strong polar solvent ACN, medium polar solvent CF, and weak polar solvent CYH, are taken as variables. Through the analysis of bond length, bond angle, absorption fluorescence property, FMO, infrared (IR) vibration analysis, natural bond orbital (NBO) distribution, and potential energy curve (PEC), the ESIPT property of AcHAQ is analyzed, hoping to provide theoretical support for the solvent photochromic effect of organic molecules.

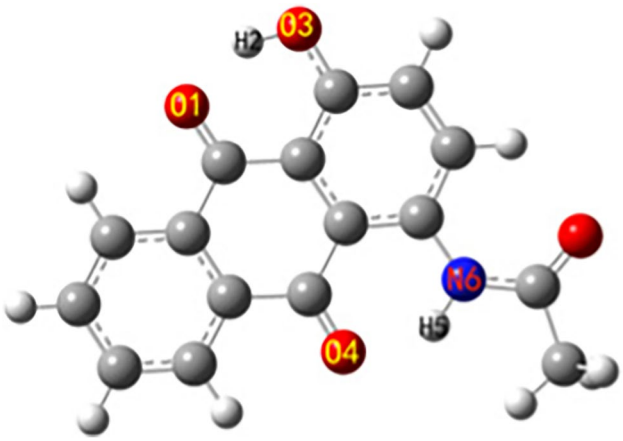

Fig. 1 The molecular configuration of AcHAQ. The significant atoms were numbered

The relevant atoms involved in the intramolecular proton transfer reaction in the excited state were numbered and shown in Fig. 1 to facilitate our subsequent discussion and analysis. The molecule contains two intramolecular hydrogen bonds O_1-H_2 bond and O_4-H_5 bond, that is, there are two positions where the ESIPT process may occur. Therefore, we consider that there are three types of ESIPT reactions: type I: H_2 is transferred from O_3 to O_1, but H_5 does not transfer; type II: H_5 is transferred from N_6 to O_4, and H_2 does not transfer; type III: H_2 and H_5 occur simultaneously transfer. On the other hand, the strength of the intramolecular hydrogen bonds of AcHAQ changes under different solvent polarities, which will affect the ESIPT reaction. Therefore, this paper mainly focuses on two main points to study the ESIPT characteristics of AcHAQ: First, what kind of situation does the ESIPT reaction of AcHAQ belong to? Second, what effect does the solvent polarity have on the ESIPT reaction of AcHAQ?

Methods

The ground-state and excited-state structures of AcHAQ in acetonitrile (ACN), chloroform (CF), and cyclohexane (CYH) were separately optimized under the DFT and TD-DFT methods. Becke's three-parameter hybrid exchange functional with Lee–Yang–Parr gradient-corrected correlation (B3LYP functional) and the 6–311 + + G(d) were utilized in both the DFT and TD-DFT methods [25–27]. It should be mentioned that there was no constrain to all the geometric parameters during optimization processes, and the vibrational analysis was performed to confirm the absence of an imaginary mode in all the local minima. To better simulate surrounding environments, all of the calculations in the present work were based on the polarizable continuum model (PCM) using the integral equation formalism variant (IEFPCM). In order to choose the most suitable functional, the maximum absorption peaks of the derivative of AcHAQ, namely 1-amino-4-hydroxyanthraquinone, were calculated using seven different functionals and corresponding results are listed in Table 1. It can be found that the functional B3LYP is most consistent with experiment data [28–32]. Hence, it was chosen to calculate the spectral properties of AcHAQ. Based on the optimized structures in ground and excited states, principal bond lengths, bond angles, IR vibration spectra, NBO population, absorption, and fluorescence properties of AcHAQ in three solvents were obtained [33–35]. Moreover, to more intuitively observe the changes of the two hydrogen bond lengths and the energy change trend of the AcHAQ during the ESIPT process in three solvents, PECs

Table 1 Maximum absorption peaks (nm) computed by seven different functional and experiment data of 1-amino-4-hydroxyanthraquinone

	B3LYP	B3PW91	CAM-B3LYP	M062X	MPW1PW91	PBEPBE	ωB97XD	Exp
λ_{max}	515	515	459	456	501	580	457	522

in the ground and excited states of AcHAQ were scanned by keeping a series of set values for the O_3-H_2 bond and the N_6-H_5 bond [36, 37]. Besides, all the calculations in this work were performed based on the Gaussian 16 software package [38].

Results and discussion

Geometric configurations

We optimized the geometry of AcHAQ in three solvents with considerable polar differences, ACN, CF, and CYH, using the TD-DFT/B3LYP method, and compared the main bond parameters related to the ESIPT reaction. The bond lengths of H_2-O_1 and H_5-O_4 and bond angles of O_1-H_2-O_3 and O_4-H_5-N_6 are listed in Table 2. In the three solvents, the variation trends of the bond parameters of AcHAQ are the same. From the ground to the excited state, the bond lengths of O_1-H_2 and O_4-H_5 are shortened, but the bond length O_1-H_2 changed more greatly; the bond angles of O_1-H_2-O_3 and O_4-H_5-N_6 enlarged, but the bond angle O_1-H_2-O_3 altered more. Taking the AcHAQ in ACN as an example, a decrease of 0.069 Å occurred for the bond length O_4-H_5 upon the photoexcitation, while the bond angle O_1-H_2-O_3 enlarged from 147.5 to 152.7°. The bond length O_1-H_2 diminished from 1.634 Å in the ground state to 1.527 Å in the excited state, a decrease of 0.097 Å, and the bond angle O_4-H_5-N_6 increased from 139.1 to 143.8°. Generally speaking, the shorter the hydrogen bond length, the stronger the hydrogen bond intensity, which is more favorable for the occurrence of ESIPT reaction. Both IHB strengths of O_1···H_2 and O_4···H_5 increased, but that of O_1···H_2 strengthened more, and its bond length was shorter than that of O_4···H_5, implying that the ESIPT process prefers to occur along the O_1···H_2 IHB.

Although in the three solvents the change trends of bond parameters of AcHAQ are the same, there are differences in value, so there are different effects on the ESIPT process of AcHAQ. As the polarity of the solvent increases, that is, the solvent changes from CYH to CF and then to ACN, the bond length O_1···H_2 in the excited state gradually shortens, from 1.553 Å in CYH to 1.539 Å in CF, and then reduced to 1.527 Å in CAN, which implies that the intensity of O_1-H_2···O_3 IHB has gradually improved as the solvent polarity heightened.

Absorption and fluorescence spectra

Using the TD-DFT/B3LYP method, with 6–311 + + G(d) as the basis set, we simulated the absorption and fluorescence spectra of AcHAQ in the three solvents, ACN, CF, and CYH, as shown in Fig. 2. The transition properties of excited states of AcHAQ are listed in Table 3. Among the three solvents, the maximum absorption peaks of AcHAQ were located at 483, 487, and 489 nm, respectively. Apparently, as the solvent polarity decreases, the maximum absorption peak is red-shifted.

In addition, the highest occupied molecular orbital (HOMO) and the lowest unoccupied molecular orbital

Table 2 Obtained significant bond lengths (Å) and bond angles (°) of AcHAQ in three solvents

	State	H_2-O_3	H_2-O_1	O_1-H_2-O_3	H_5-O_4	N_6-H_5-O_4
ACN	S_0	0.992	1.634	147.5	1.757	139.0
	S_1	1.020	1.527	152.6	1.686	143.8
CF	S_0	0.992	1.638	147.3	1.756	139.1
	S_1	1.017	1.539	152.2	1.686	143.9
CYH	S_0	0.991	1.643	147.0	1.755	139.1
	S_1	1.014	1.553	151.6	1.687	143.8

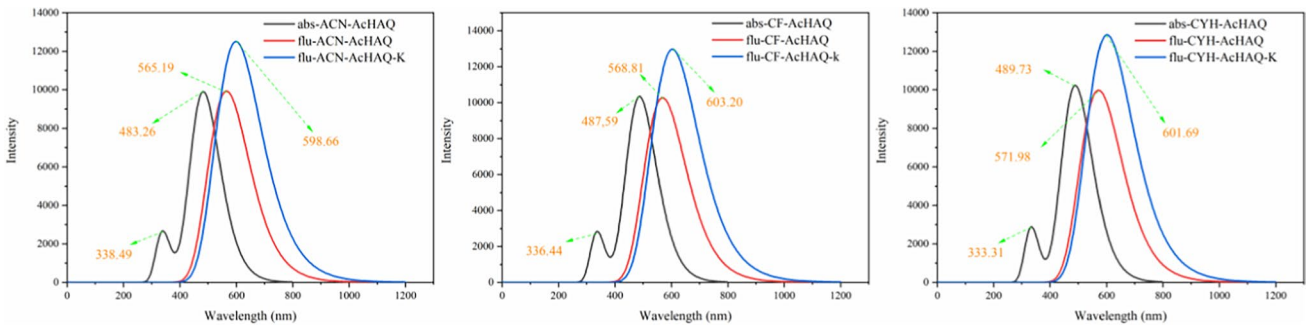

Fig. 2 Absoprtion and fluorescence spectra of AcHAQ in three solvents. Herein, K means the proton transfer tautomer

Table 3 Calculated transition properties of AcHAQ in three different solvents via TD-DFT/B3LYP/6–311 + + G(d) method

	State	E (nm)	Contribution MO	Strength *f*
ACN	S_1	483	(70.409%)H→L	0.2445
	S_2	413	(61.540%)H-1→L	0.0000
	S_3	360	(61.368%)H-6→L	0.0000
	S_4	358	(60.980%)H-2→L	0.0048
	S_5	344	(54.198%)H-4→L	0.0000
	S_6	338	(61.776%)H-3→L	0.0621
CF	S_1	487	(70.439%)H→L	0.2553
	S_2	415	(61.321%)H-1→L	0.0000
	S_3	362	(58.311%)H-6→L	0.0000
	S_4	356	(65.845%)H-2→L	0.0046
	S_5	344	(50.958%)H-4→L	0.0000
	S_6	336	(66.819%)H-3→L	0.0664
CYH	S_1	489	(70.457%)H→L	0.2524
	S_2	418	(61.255%)H-1→L	0.0000
	S_3	364	(54.320%)H-5→L	0.0000
	S_4	354	(67.326%)H-2→L	0.0043
	S_5	350	(46.998%)H-4→L	0.0000
	S_6	333	(68.417%)H-3→L	0.0679

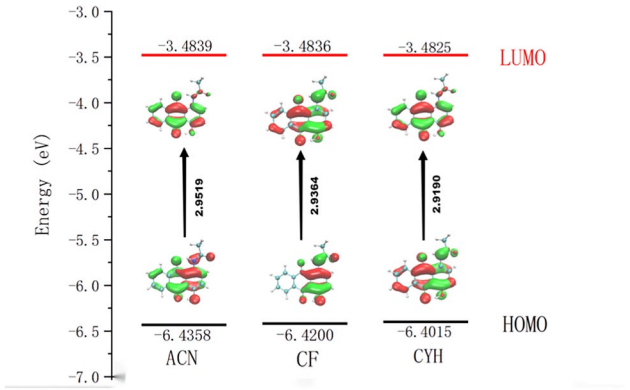

Fig. 3 Frontier molecular orbitals (FMOs) and corresponding energy gap values (eV) of AcHAQ in three solvents

(LUMO) were also calculated and exhibited in Fig. 3. It can be found that the S_1 states of AcHAQ show π→π* features, in which the HOMO and LUMO exhibit the π and π* properties, respectively. From Fig. 3, it can be seen that the HOMO–LUMO gap of AcHAQ in ACN is 2.951 eV, which is higher than 2.936 eV in CF and 2.919 eV in CYH. Table 4 lists the fluorescence properties of AcHAQ in three different solvents. The fluorescence peaks of AcHAQ in three different solvents of ACN, CF, and CYH are 565, 568, and 571 nm, respectively, and the corresponding stokes shifts are 81, 81, and 82 nm, respectively. The above calculation results show that the change of solvent polarity has a significant effect on the absorption and fluorescence properties of AcHAQ.

Table 4 Fluorescence properties of AcHAQ in three solvents. Herein, K means the proton transfer tautomer

	State	Energy (eV)	λ_{flu} (nm)	Contribution MO	Strength *f*
ACN	S_1	2.193	565	(70.805%)H→L	0.2452
	K	2.071	598	(71.390%)H→L	0.3087
CF	S_1	2.179	568	(70.787%)H→L	0.2535
	K	2.055	603	(71.365%)H→L	0.3201
CYH	S_1	2.167	571	(70.795%)H→L	0.2463
	K	2.060	601	(71.354%)H→L	0.3173

Table 5 Calculated stretching vibrational models of O_3–H_2 and N_6–H_5 in three different solvents at S_0 and S_1 states (cm^{-1})

		ACN	CF	CYH
S_0	O_3–H_2	3227	3236	3252
	N_6–H_5	3402	3404	3404
S_1	O_3–H_2	2732	2788	2852
	N_6–H_5	3156	3172	3180

IR vibrational spectra

It is well accepted that the IHB strengthening or weakening could be also revealed via evaluating the IR vibrational spectra shifts of characteristic vibrational modes involved in the IHBs [39, 40]. We have also calculated the IR vibrational spectra of AcHAQ and exhibited the stretching vibrational modes of O_3-H_2 and N_6-H_5 as shown in Table 5. It can be clearly seen that, after the photoexcitation, two vibrational peaks of AcHAQ have apparent red shifts, which indicates that the two hydrogen bonds have been strengthened. We have also noticed that the red-shift values for O_3-H_2 hydrogen are above 400 cm^{-1}, while that of the N_6-H_5 hydrogen bond do not exceed 200 cm^{-1}. The enhancement of the O_1···H_2-O_3 hydrogen bond is more robust than the O_4···H_5-N_6 hydrogen bond. The magnitude of the bond strengthening is much greater, and the intramolecular proton transfer is more likely to occur.

Among the three solvents, the red-shift value of the O_3-H_2 hydrogen bond is 495 cm^{-1} in ACN, 448 cm^{-1} in CF, and 400 cm^{-1} in CYH. It can be found that when the AcHAQ transitions from the S_0 to the S_1 state, the red-shift value of the IR vibrational peak for the O_1···H_2-O_3 hydrogen bond increases with the increase of the solvent polarity, indicating that IHBs are more stronger in ACN, which is beneficial to the occurrence of the ESIPT process and is consistent with the results obtained from geometric parameters.

NBO analysis

Investigating the charge distribution during the optical excitation process has always been an effective way to analyze the molecular dynamic [20, 41]. The charge distribution on O_1, O_3, O_4, and N_6 atoms of AcHAQ in the S_0 and S_1 states was calculated based on NBO populations and listed in Table 6. For all the studied solvents, the charge localized on the O_3 and N_6 atoms was decreased, while that on the O_1 and O_4 was increased. For instance, the charge distributed on the O_3 and N_6 of AcHAQ in ACN has lessened from − 0.677 a.u. and − 0.612 a.u. in the S_0 state to − 0.626 a.u. and − 0.547 a.u. in the S_1 state, indicating that the capacity of the O_3 and N_6 atoms to bind the proton has been weakened upon the photoexcitation. Besides, the charge distribution on the O_1 and O_4 atoms in ACN has enlarged from − 0.634 a.u. and − 0.619 a.u. in the S_0 state to − 0.667 a.u. and − 0.659 a.u. in the S_1 state, which implies the enhanced ability of the O_1 and O_4 atom to attract protons, thereby triggering the ESIPT behavior.

PESs

To further explore the ESIPT mechanism in the three solvents, we scanned the PESs of AcHAQ via varying the O_3-H_2 and N_6-H_5 distance and allowing all other degrees of freedom to relax freely towards the minimum energy as shown in Fig. 4. As presented in Fig. 4, the Z-direction indicates the energy of the molecule, and the positive direction of the left coordinate is the direction of O_3-H_2 bond lengthening, which represents the reaction process of proton transfer from O_3 to O_1, i.e., type I reaction. Moreover, the positive direction of the right coordinate is the direction of N_6-H_5 bond lengthening, which represents the reaction process of proton transfer from N_6 to O_4, i.e., type II reaction.

It can be found from Fig. 4 that the energy increases monotonically with the elongation of O_3-H_2 and N_6-H_5 bonds, which indicates that proton transfer processes of AcHAQ in the three solvents cannot occur in the ground state. This is well understood. The AcHAQ is in the low-energy S_0 state, and the hydrogen bond is relatively stable, making it difficult for proton transfer reactions to occur. But when we looked at the AcHAQ in the S_1 state, the situation became different, as shown in Fig. 5. First, in different solvents, the energy barrier exists only in the direction of the type I reaction, indicating that the intramolecular proton transfer reaction of the excited state of the AcHAQ only occurs between the O_1 and O_3 atoms. Second, we found that the energy barrier for the type I reaction is the lowest in ACN, followed by CF, and highest in CYH, that is, the ESIPT reaction is more likely to occur in strongly polar solvents.

Table 6 NBO charge distribution (a.u.) of the O_1, O_3, O_4, and N_6 atoms in the three solvents at the S_0 and S_1 states

		O_1	O_3	O_4	N_6
ACN	S_0	− 0.634	− 0.677	− 0.619	− 0.612
	S_1	− 0.667	− 0.626	− 0.659	− 0.547
CF	S_0	− 0.628	− 0.671	− 0.616	− 0.614
	S_1	− 0.653	− 0.622	− 0.649	− 0.552
CYH	S_0	− 0.622	− 0.665	− 0.612	− 0.617
	S_1	− 0.640	− 0.620	− 0.639	− 0.557

Conclusion

In this work, three different solvents, ACN, CF, and CYH, were selected to change the polarity of the solvent environment where the AcHAQ was located so as to study the influence of the solvent effect on the ESIPT process of the AcHAQ. Using DFT and TD-DFT, the ESIPT mechanism of AcHAQ in solvents of different polarities was deeply studied, and the main parameters closely related to the ESIPT process, such as bond lengths and bond angles, were obtained. Absorption and fluorescence spectra, FMOs, IR vibrational spectra, NBO populations, and PESs were

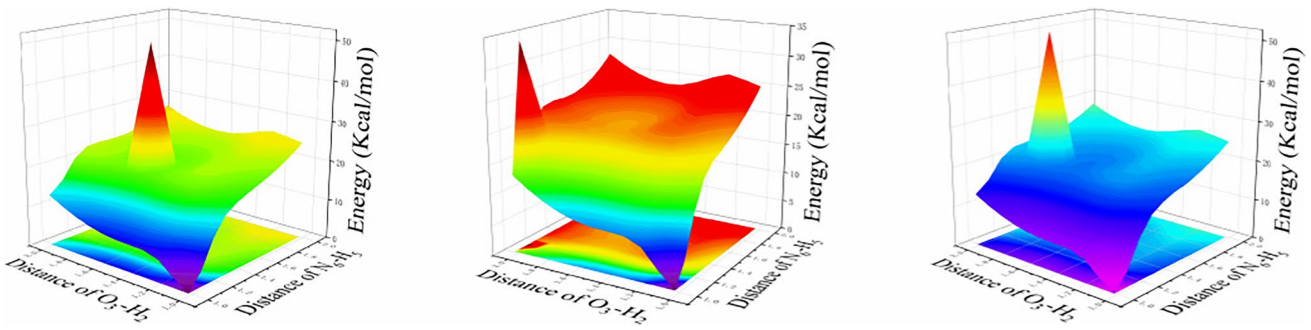

Fig. 4 Potential energy surfaces (PESs) for the S_0 state of AcHAQ in three solvents along with the increasing bond lengths of O_3–H_2 and N_6–H_5

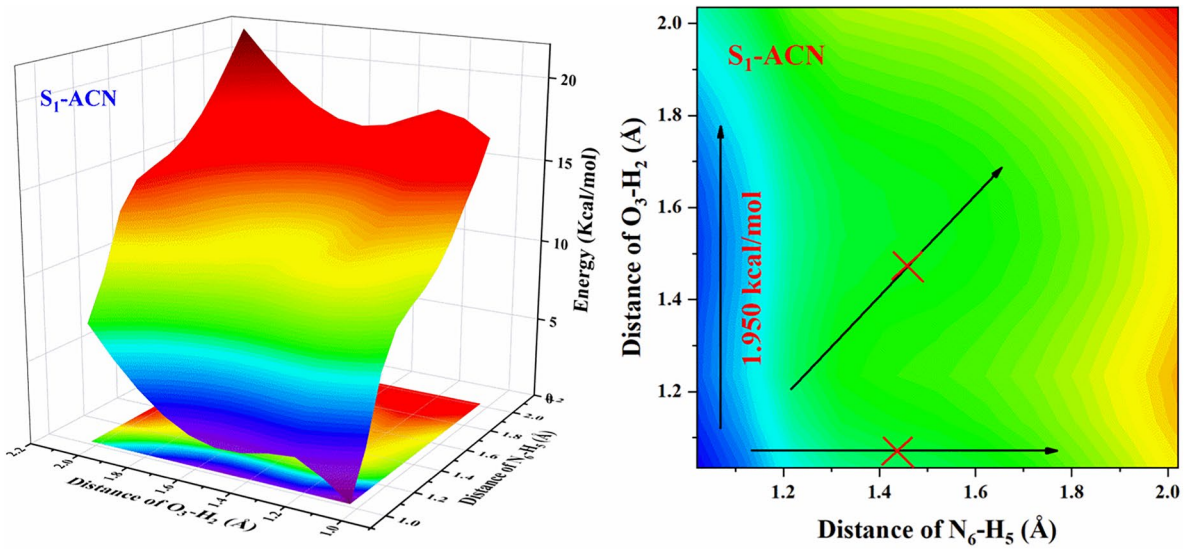
S1-ACN
Energy (Kcal/mol)
Distance of O3-H2 (Å)
Distance of N6-H5 (Å)
S1-ACN
1.950 kcal/mol
Distance of O3-H2 (Å)
Distance of N6-H5 (Å)

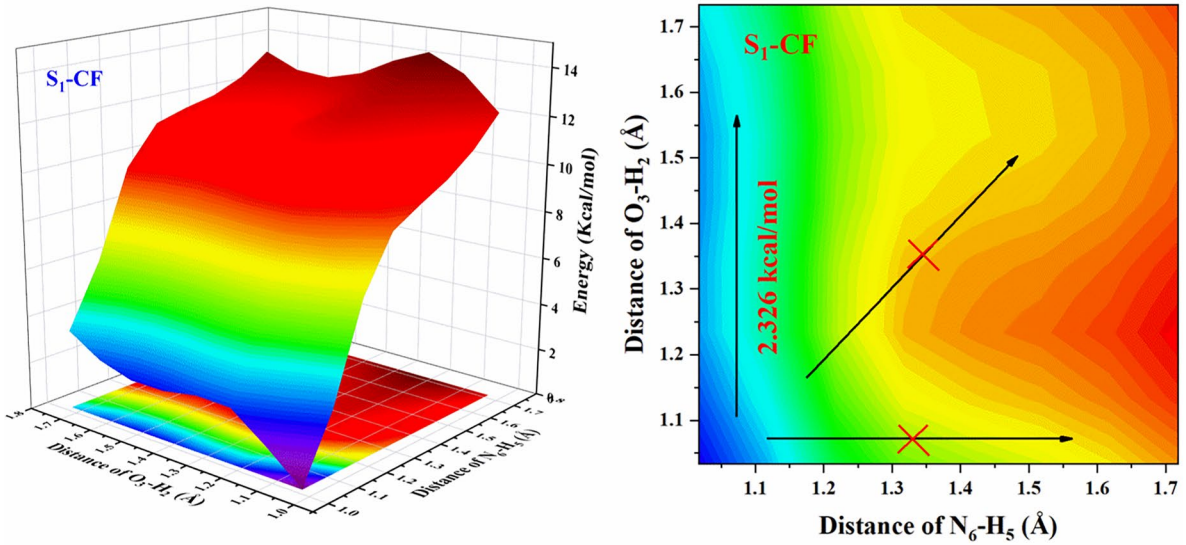
S1-CF
Energy (Kcal/mol)
Distance of O3-H2 (Å)
Distance of N6-H5 (Å)
S1-CF
2.326 kcal/mol
Distance of O3-H2 (Å)
Distance of N6-H5 (Å)

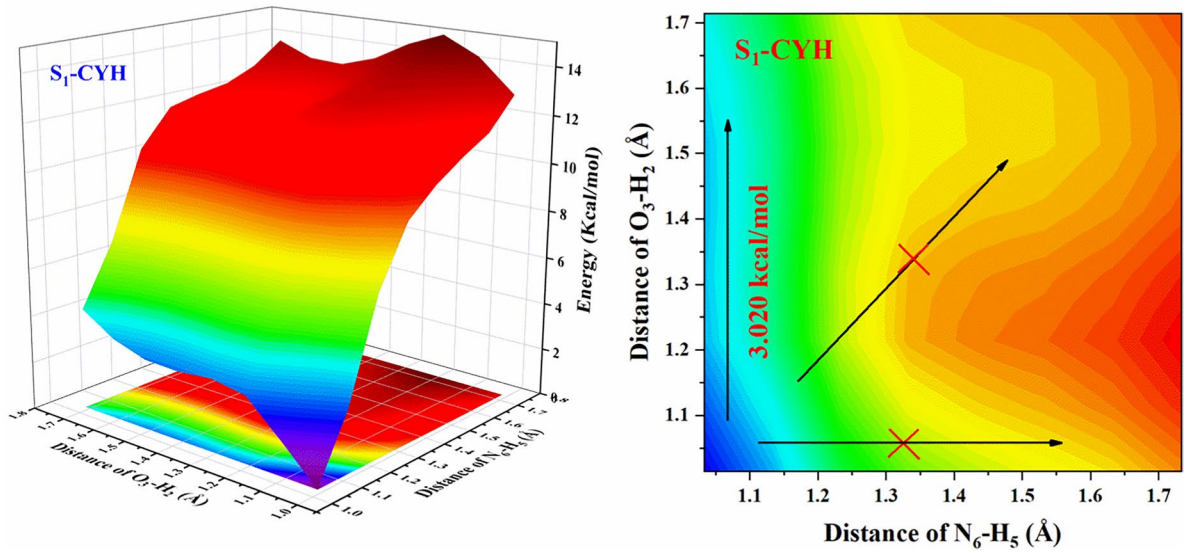
S1-CYH
Energy (Kcal/mol)
Distance of O3-H2 (Å)
Distance of N6-H5 (Å)
S1-CYH
3.020 kcal/mol
Distance of O3-H2 (Å)
Distance of N6-H5 (Å)

◂**Fig. 5** Potential energy surfaces (PESs) for the S_1 state of AcHAQ in three solvents along with the increasing bond lengths of O_3–H_2 and N_6–H_5

analyzed. Finally, it is concluded that the ESIPT process of AcHAQ is mainly a type I reaction, and the type II and type III reactions hardly occur. Besides, AcHAQ is more likely to undergo ESIPT reaction in ACN, while it is difficult to proceed in CYH, indicating that strong polar solvents have a reinforcing effect on the IHB of the AcHAQ, thereby promoting the ESIPT process. This conclusion provides a theoretical basis for regulating the luminescence properties of organic molecules by changing the polarity of the solvent.

Author contribution Xin Xu: conceptualization, data curation, writing—original draft. Zeran Zhang: investigation, writing—review and editing. Yajie Zhang, Linyue Jin, and Qian Cheng: writing—review and editing. Fang Liu: conceptualization, methodology, writing—review and editing, resources. Chaofan Sun: conceptualization, methodology, investigation, software, writing—review and editing, resources.

Funding This work was financially supported by the Innovation Training Project Program of Heilongjiang Province (No. S202210225053) and the Fundamental Research Funds for the Central Universities (No. 2572020BC03).

Data availability The datasets generated during and/or analyzed during the current study are available from the corresponding author on reasonable request.

Code availability Not applicable.

Declarations

Conflict of interest The authors declare no competing interests.

References

1. Tang KC, Chang MJ, Lin TY et al (2011) J Am Chem Soc 133:17738
2. Chen L, Ye JW, Wang HP et al (2017) Nat Commun 8:15985
3. Yang XF, Huang Q, Zhong YG et al (2014) Chem Sci 5:2177
4. Wu LL, Sedgwick AC, Sun XL, Bull SD, He XP, James TD (2019) Acc Chem Res 52:2582
5. Padalkar VS, Seki S (2016) Chem Soc Rev 45:169
6. Zhang W, Yan YL, Gu JM, Yao JN, Zhao YS (2015) Angew Chem Int Ed 54:7125
7. Kim D, Jeong K, Kwon JE et al (2019) Nat Commun 10:3089
8. Wei GQ, Yu Y, Zhuo MP, Wang XD, Liao LS (2020) J Mater Chem C 8:11916
9. Qian HL, Dai C, Yang CX, Yan XP (2017) ACS Appl Mater Interfaces 9:24999
10. Boonkitpatarakul K, Wang JF, Niamnont N et al (2016) ACS Sens 1:144
11. Azarias C, Budzak S, Laurent AD, Ulrich G, Jacquemin D (2016) Chem Sci 7:3763
12. Tian MG, Ma YY, Lin WY (2019) Acc Chem Res 52:2147
13. Shang CJ, Cao YJ, Sun CF, Zhao HF (2022) Phys Chem Chem Phys 24:8453
14. Dutta S, Mandal D (2022) J Mol Liq 361:119651
15. Han JH, Cao BF, Li Y et al (2020) Spectrochim Acta, Part A 231:118086
16. Cao YJ, Yu XR, Sun CF, Cui JA (2022) Int J Mol Sci 23:2132
17. Niu YH, Wang R, Shao PL, Wang YX, Zhang YR (2018) Chem - Eur J 24:16670
18. Yang YF, Luo X, Ma FC, Li YQ (2021) Spectrochim Acta, Part A 250:119375
19. Sun CF, Li Y, Li B et al (2020) J Mol Liq 297:111937
20. Sun CF, Zhao HF, Liu XC, Yin H, Shi Y (2018) Org Chem Front 5:3435
21. Yang WY, Lai RC, Wu JJ et al (2022) Adv Funct Mater 32:2204129
22. Zhang YJ, Shang CJ, Cao YJ, Ma M, Sun CF (2022) Spectrochim Acta, Part A 280:121559
23. Li Q, Wan Y, Zhou Q et al (2022) Spectrochim Acta, Part A 272:120953
24. Yu XR, Cao YN, Li YZ, Cui JA, Sun CF (2022) J Mol Struct 1250:131923
25. Tirado-Rives J, Jorgensen WL (2008) J Chem Theory Comput 4:297
26. Cossi M, Barone V (2001) J Chem Phys 115:4708
27. Adamo C, Jacquemin D (2013) Chem Soc Rev 42:845
28. Zhang J, Lalevee J, Hill NS et al (2018) Macromolecules 51:8165
29. Durant JL (1996) Chem Phys Lett 256:595
30. Jacquemin D, Wathelet V, Perpete EA, Adamo C (2009) J Chem Theory Comput 5:2420
31. Jacquemin D, Perpete EA, Scuseria GE, Ciofini I, Adamo C (2008) J Chem Theory Comput 4:123
32. Valdes H, Pluhackova K, Pitonak M, Rezac J, Hobza P (2008) Phys Chem Chem Phys 10:2747
33. Zhao JF, Chen JS, Liu JY, Hoffmann MR (2015) Phys Chem Chem Phys 17:11990
34. Zhou PW, Han K (2018) Acc Chem Res 51:1681
35. Yin H, Li H, Xia GM et al (2016) Sci Rep 6:19774
36. Li CZ, Ma C, Li DL, Liu YF (2016) J Lumin 172:29
37. Li YQ, Ma YZ, Yang YF, Shi W, Lan RF, Guo Q (2018) Phys Chem Chem Phys 20:4208
38. Frisch MJ, Trucks GW, Schlegel HB, Scuseria GE, Robb MA, Cheeseman JR, Scalmani G, Barone V, Petersson GA, Nakatsuji H, Li X, Caricato M, Marenich AV, Bloino J, Janesko BG, Gomperts R, Mennucci B, Hratchian HP, Ortiz JV, Izmaylov AF, Sonnenberg JL, Williams DF, Lipparini F, Egidi F, Goings J, Peng B, Petrone A, Henderson T, Ranasinghe D, Zakrzewski VG, Gao J, Rega N, Zheng G, Liang W, Hada M, Ehara M, Toyota K, Fukuda R, Hasegawa J, Ishida M, Nakajima T, Honda Y, Kitao O, Nakai H, Vreven T, Throssell K, Montgomery JA Jr, Peralta JE, Ogliaro F, Bearpark MJ, Heyd JJ, Brothers EN, Kudin KN, Staroverov VN, Keith TA, Kobayashi R, Normand J, Raghavachari K, Rendell AP, Burant JC, Iyengar SS, Tomasi J, Cossi M, Millam JM, Klene M, Adamo C, Cammi R, Ochterski JW, Martin RL, Morokuma K, Farkas O, Foresman JB, Fox DJ (2016) Gaussian 16. Gaussian Inc, Wallingford, CT, USA
39. Liang NQ, Kuwata S, Ishige R, Ando S (2021) Mater Chem Front 6:24
40. Li Y, Sun CF, Han JH et al (2020) J Lumin 221:117110
41. Inamdar SR, Mannekutla JR, Sannaikar MS, Wari MN, Mulimani BG, Savadatti MI (2018) J Mol Liq 268:66